
AN EMPIRICAL EXPLORATION OF DEEP RECURRENT CONNECTIONS AND MEMORY CELLS USING NEURO-EVOLUTION

Travis J. Desell
tjdvse@rit.edu

AbdElRahman A. ElSaid
aelsaid@mail.rit.edu

Alexander G. Ororbia
ago@cs.rit.edu

Golisano College of Computing and Information Sciences
Rochester Institute of Technology
Rochester, NY 14623

Neuro-evolution and neural architecture search algorithms have gained increasing interest due to the challenges involved in designing optimal artificial neural networks (ANNs). While these algorithms have been shown to possess the potential to outperform the best human crafted architectures, a less common use of them is as a tool for analysis of ANN structural components and connectivity structures. In this work, we focus on this particular use-case to develop a rigorous examination and comparison framework for analyzing recurrent neural networks (RNNs) applied to time series prediction using the novel neuro-evolutionary process known as Evolutionary eXploration of Augmenting Memory Models (EXAMM). Specifically, we use our EXAMM-based analysis to investigate the capabilities of recurrent memory cells and the generalization ability afforded by various complex recurrent connectivity patterns that span one or more steps in time, i.e., deep recurrent connections. EXAMM, in this study, was used to train over 10.56 million RNNs in 5,280 repeated experiments with varying components. While many modern, often hand-crafted RNNs rely on complex memory cells (which have internal recurrent connections that only span a single time step) operating under the assumption that these sufficiently latch information and handle long term dependencies, our results show that networks evolved with deep recurrent connections perform significantly better than those without. More importantly, in some cases, the best performing RNNs consisted of only simple neurons and deep time skip connections, *without any memory cells*. These results strongly suggest that utilizing deep time skip connections in RNNs for time series data prediction not only deserves further, dedicated study, but also demonstrate the potential of neuro-evolution as a means to better study, understand, and train effective RNNs.

1 Introduction

Neural architecture search poses a challenging problem since the possible search space for finding optimal or quasi-optimal architectures is massive. For the case of recurrent neural networks (RNNs), this problem is further confounded by the fact that every node in its architecture can be potentially connected to any other node via a recurrent connection which passes information stored in a vector history to the current time step. Complexity is further increased when one considers that recurrent connections could explicitly connect information from any time step $< t$ in the history of the sequence processed so far to step t , improving memory retention through time delays. Most modern-day RNNs simplify the recurrent connectivity structure and instead improve retention by utilizing memory cells such as Δ -RNN units [1], gated recurrent units (GRUs) [2], long short-term memory cells (LSTMs) [3], minimal gated units (MGUs) [4], and update gate RNN cells (UGRNNs) [5]. The use of memory cells, as opposed to investigating the use of denser temporal/recurrent connectivity structures, is popular largely under the assumption that, while the recurrent synapses that define a cell only explicitly connect $t - 1$ to t , their latch-like behavior is sufficient for capturing enough information about the sequence observed so far when making predictions of what will come next. Nonetheless, RNNs still struggle to effectively learn long-term dependencies in temporal data and the quest for the optimal memory cell continues to this day [6, 7, 8, 9, 1, 10].

There, however, exists a body of literature that suggests that recurrent connections which skip more than a single time step, which we will coin as *deep recurrent connections*, can play an important role in allowing an RNN to more effectively capture long-term temporal dependencies. This research dates back to Lin *et al*'s development of NARX (Nonlinear AutoRegressive eXogenous Model) neural networks with increasing embedded memory orders (EMOs) or time windows [11, 12], which involved adding recurrent connections up to a specified number time skips. Further

work went on to show that the order of a NARX network is crucial in determining how well it will perform – when the EMO of a NARX model matches the order of an unknown target recursive system strong and robust generalization is achieved [13, 14]. Diaconescu later utilized these EMO-based NARX networks to predict chaotic time series data, with best results found in the EMO ranges of 12 to 30, which are significantly large time skips [15]. More generally, it has been expressed in classical literature that skip connections can substantially express the computational abilities of artificial neural networks (ANNs) [16]. Yet, modern popular ANNs have only taken advantage of feedforward skip connections [17], including RNNs [18, 19], with a few notable exceptions [20].

Findings for RNNs with deep recurrent connections are also not limited to Lin *et al*'s EMO NARX networks. Chen and Chaudhari developed a segmented-memory recurrent neural network (SMRNN) [21], which utilizes a two layer recurrent structure which first passes input symbols to a symbol layer, and then connects the symbol layers to a segmentation layer. This work showed that intervals $10 \leq d \leq 50$ provided the best results on this data, as a lower d required more computation each iteration (the segmentation was used too frequently) slowing convergence, and at higher values of d it approximated a conventional RNN (that did not use a segmentation layer). The segment interval d operates similarly to a deep recurrent connection; it passes information from past states further forward along the unrolled network. It was shown that SMRNN outperformed both LSTM and Elman RNNs on the latching problem. ElSaid *et al* later utilized time-windowed LSTM RNNs to predict engine vibration in time series data gathered from aircraft flight data recorders [22, 23]. This work investigated a number of architectures and found that a two-level system with an EMO/time window of order 10 provided good predictions of engine vibration up to 20 seconds in the future. This was a challenging problem due to the spiking nature of engine vibration, yet this architecture significantly outperformed time-windowed NARX models, Nonlinear Output Error (NOE), and the Nonlinear Box–Jenkins (NBJ) models.

In this work, we further investigate power of deep recurrent connections in comparison to memory cells by taking a rather unconventional approach to the analysis, using an neuro-evolutionary algorithm we call EXAMM (Evolutionary eXploration of Augmenting Memory Models) [24]. Instead of simply testing a few hand-crafted RNNs with and without deep recurrent connections composed of different kinds of memory cells, neuro-evolution was used to select and mix the architectural components as well as decide the depth and density of the connectivity patterns, facilitating an exploration of the expansive, combinatorial search space when accounting for the many different components and dimensions one could explore – yielding a more rigorous, comprehensive yet automated examination. A variety of experiments were performed evolving RNNs consisting of simple neurons or memory cells, e.g., LSTM, GRU, MGU, UGRNN, Δ -RNN cells, as well as exploring the option of using deep recurrent connections or not, of varying degree and intensity. RNNs were evolved with EXAMM to perform time series data prediction on four real world benchmark problems. In total, 10.56 million RNNs were trained to collect the results we report in this study.

The findings of our EXAMM-driven experimentation uncovered that networks evolved with deep recurrent connections perform significantly better than those without, and, notably, in some cases, the best performing RNNs consisted of only simple neurons with deep recurrent connections (*i.e.*, no memory cells). These results strongly suggest that utilizing deep recurrent connections in RNNs for time series data prediction not only warrants further study, but also demonstrates that neuro-evolution is a potentially powerful tool for studying, understanding, and training effective RNNs. Another salient result from our findings is that, for time series prediction, the relatively new Δ -RNN cell performs better and more reliably than other memory cells.

2 Evolving Recurrent Neural Networks

Neuro-evolution, or the use of artificial evolutionary processes (such as genetic algorithms [25]) to automate the design of artificial neural networks (ANNs), has been well applied to feed forward ANNs for tasks involving static inputs, including convolutional variants [26, 27, 28, 29, 30, 31]. However, significantly less effort has been put into exploring the evolution of recurrent memory structures that operate with complex sequences of data points.

Despite the current lack of focus on RNNs, several neuro-evolution methods have been proposed evolving RNN topologies (along with weight values themselves) with NeuroEvolution of Augmenting Topologies (NEAT) [30] perhaps being the most well-known. Recent work by Rawal and Miikkulainen investigated an information maximization objective [32] strategy for evolving RNNs, which essentially operates similarly to NEAT except with LSTM cells being used instead of simple (traditional) neurons. Research centered around this line of NEAT-based approaches has also explored the use of a tree-based encoding [33] to evolve recurrent cellular structures within fixed architectures composed of multiple layers of the evolved cell types. More recently, work by Camero *et al* has shown that a Mean Absolute Error (MAE) random sampling strategy can provide good estimates of RNN performance [34], successfully incorporating it into an LSTM-RNN neuro-evolution strategy [35]. However, none of this prior work has investigated the evolution deep recurrent connectivity structures nor focused on using a powerful evolutionary strategy such as EXAMM as an empirical analysis tool for RNNs.

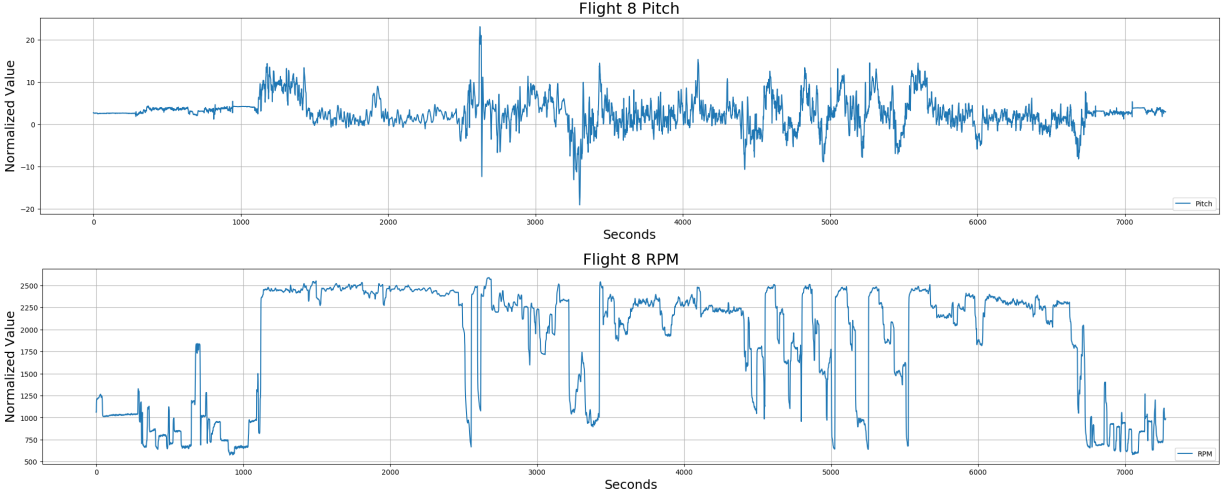


Figure 1: Example parameters pitch (top) and RPM (bottom) of Flight 8 from the NGAFID dataset.

With respect to other nature-inspired metaheuristic approaches for evolving RNNs, ant colony optimization (ACO) has also been investigated [36] as a way to select which connections should be used but only for single time-step Elman RNNs. ACO has also been used to reduce the number of trainable connections in a fixed time-windowed LSTM architecture by half while providing significantly improved prediction of engine vibration [37].

For this study, EXAMM was selected as the RNN analysis algorithm for a number of reasons. First, this procedure progressively grows larger ANNs in a manner similar to NEAT which stands in contrast to current ACO-based approaches, which have been often restricted to operating within a fixed neural topology. Furthermore, in contrast to the well-known NEAT, EXAMM utilizes higher order node-level mutation operations, Lamarckian weight initialization (or the reuse of parental weights), and back-propagation of errors (backprop) [38] to conduct local search, the combination of which has been shown to speed up both ANN training as well as the overall evolutionary process. Unlike the work by Rawal and Miikkulainen, EXAMM operates with an easily-extensible suite of memory cells, including LSTM, GRU, MGU, UGRNN, Δ -RNN cells and, more importantly, has the natural ability to evolve deep recurrent connections over large, variable time lags. In prior work it has also been shown to more quickly and reliably evolve RNNs in parallel than training traditional layered RNNs sequentially [39]. For detailed EXAMM implementation details we refer the reader to [24].

3 Experimental Data

This experimental study utilized two open-access real-world data sets as benchmark problems for evolving RNNs that can predict four different time series parameters. The first dataset comes from a selection of 10 flights worth of data taken from the National General Aviation Flight Information Database (NGAFID) and the other comes from data collected from 12 burners of a coal-fired power plant. Both datasets are multivariate (with 26 and 12 parameters, respectively), non-seasonal, and the parameter recordings are not independent. Furthermore, the underlying temporal sequences are quite long – the aviation time series range from 1 to 3 hours worth of per-second data while the power plant data consists of 10 days worth of per-minute readings. To the authors’ knowledge, other real world time series data sets of this size and at this scale are not freely available. These datasets are freely provided in the EXAMM github repository¹.

3.1 Aviation Flight Recorder Data

Each of the 10 flight data files last over an hour and consist of per-second data recordings from 26 parameters, including engine parameters such as engine cylinder head temperatures, gasket temperatures, oil temperature and pressure, and rotations per minute (RPM); flight parameters such as altitude above ground level, indicated air speed, lateral and normal acceleration, pitch, and roll; and environmental parameters such as outside air temperature and wind speed. The data is provided raw and without any normalization applied.

¹<https://github.com/travisesell/exact>

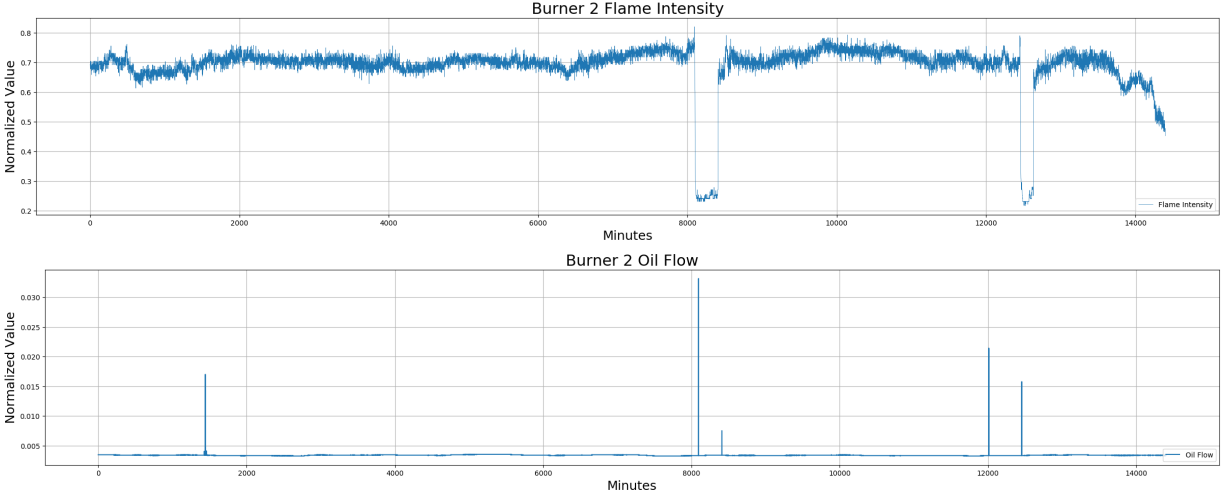


Figure 2: Example parameters for Burner #2 from the coal plant dataset: flame intensity (top) and fuel flow (bottom).

RPM and *pitch* were selected as prediction parameters from the aviation data since *RPM* is a product of engine activity, with other engine-related parameters being correlated. *Pitch* itself is directly influenced by pilot controls. As a result, both of these target variables are particularly challenging to predict. Figure 1 provides an example of the *RPM* and *pitch* time series from Flight 8 of this dataset. In addition, the *pitch* parameter represents how many degrees above or below horizontal the aircraft is angled. As a result, the parameter typically remains steady around a value of 0, however, it increases or decreases depending on whether or not the aircraft is angled to fly upward or downward, based on pilot controls and external conditions. On the other hand, *RPM* will mostly vary between an idling speed, i.e., if the plane is on the ground, and a flight speed, with some variation between takeoff and landing. Since the majority of the flights in NGAFID (and, by extension, all of the flights in the provided sample) are student training flights, multiple practice takeoffs and landings can be found. This results in two different types of time series, both of which are dependent on the other flight parameters but each with highly different characteristics – creating excellent time series benchmarks for RNNs.

3.2 Coal-fired Power Plant Data

This dataset consists of 10 days of per-minute data readings extracted from 12 out of a coal plant’s set of burners. Each of these 12 data files contains 12 parameters of time series data: Conditioner Inlet Temp, Conditioner Outlet Temp, Coal Feeder Rate, Primary Air Flow, Primary Air Split, System Secondary Air Flow Total, Secondary Air Flow, Secondary Air Split, Tertiary Air Split, Total Combined Air Flow, Supplementary Fuel Flow, and Main Flame Intensity. This data was normalized to the range $[0, 1]$, which serves furthermore as a data anonymization step.

For the coal plant data, *main flame intensity* and *supplementary fuel flow* were selected as parameters of interest. Figure 2 provides examples of these two parameters from Burner # 2 found in the dataset. Main flame intensity is mostly a product of conditions within the burner and parameters related to coal quality which causes it to vary over time. However sometimes planned outages occur or conditions in the burner deteriorate so badly that it is temporarily shut down. In these cases, sharp spikes occur during the shutdown, which last for an unspecified period of time before the burner turns back on again and the parameter (value) sharply increases. The burners can also potentially operate at different output levels, depending on power generation needs. As a result, step-wise behavior is observed.

On the other hand, supplementary fuel flow remains fairly constant. Nonetheless, it yields sudden and drastic spikes in response to decisions made by plant operators. When conditions in the burners become poor due to coal quality or other effects, the operator may need to provide supplementary fuel to prevent the burner from going into shutdown. Of particular interest is if an RNN can successfully detect these spikes given the conditions of the other parameters. Similar the key parameters (*RPM* and *pitch*) selected in the NGAFID data, main flame intensity is mostly a product of conditions within the (coal) burner while supplementary fuel flow is more directly controlled by human operators. Despite these similarities, however, the characteristics of these time series are different from each other as well as from the NGAFID flight data, providing additional, unique benchmark prediction challenges.

4 Results

4.1 Experiments

The first set of (5) experiments only permitted the use of a single memory cell type, *i.e.*, exclusively Δ -RNN, GRU, LSTM, MGU, or UGRNN (one experiment per type), and no simple neurons. All of these experiments only allowed the generation of feedforward connections between cells (these experiments were denoted as *delta*, *gru*, *lstm*, *mgu* or *ugrnn*). The second set of (2) experiments were conducted where the first one only permitted the use of simple neurons and feedforward connections (denoted as *simple*) while the second permitted EXAMM to make use of feedforward connections and simple neurons as well as the choice of any memory cell type (denoted as *all*). The next set of experiments (5) were identical to the first set with the key exception that EXAMM could choose either between simple neurons and one specified specific memory cell type (these experiments are appended with a *+simple*, *i.e.*, *lstm+simple*). The final set of (12) experiments consisted of taking the setting of each of the prior 12 (5 + 2 + 5) runs and re-ran them but with the modification that EXAMM was permitted to generate deep recurrent connections of varying time delays (these runs are appended with a *+rec*).

This full set of (24) experiments was conducted for each of the four prediction parameters, *i.e.*, RPM, pitch, main flame intensity, and supplementary fuel flow. K -fold cross validation was carried out for each prediction parameter, with a fold size of 2. This resulted in 5 folds for the NGAFID data (as it had 10 flight data files), and 6 folds for the coal plant data (as it has 12 burner data files). Each fold and EXAMM experiment was repeated 10 times. In total, each of the 24 EXAMM experiments were conducted 220 times (50 times each for the NGAFID parameter k -fold validation and 60 times each for the coal data parameter k -fold validation), for a grand total of 5,280 separate EXAMM experiments/simulations.

4.2 EXAMM and Backpropagation Hyperparameters

All RNNs were locally trained with backpropagation through time (BPTT) [40] and stochastic gradient descent (SGD) using the same hyperparameters. SGD was run with a learning rate of $\eta = 0.001$, utilizing Nesterov momentum with $mu = 0.9$. No dropout regularization was used since, in prior work, it has been shown to reduce performance when training RNNs for time series prediction [37]. For the LSTM cells that EXAMM could make use of, the forget gate bias had a value of 1.0 added to it, as [41] has shown that doing so improves training time significantly. Otherwise, RNN weights were initialized by EXAMM’s Lamarckian strategy.

To control for exploding and vanishing gradients, we apply re-scaling to the full gradient of the RNN, \vec{g} , which is one single vector of all the partial derivatives of the cost function with respect to the individual weights (in terms of a standard RNN, this amounts to flattening and concatenating all of the individual derivative matrices into one single gradient vector). Re-scaling was done in this way due to the unstructured/unlayered RNNs evolved by EXAMM. Computing the stabilized gradient proceeds formally as follows:

$$\vec{g} = \begin{cases} \vec{g} * \frac{t_h}{\|\vec{g}\|_2}, & \text{if } \|\vec{g}\|_2 > t_h \\ \vec{g} * \frac{t_l}{\|\vec{g}\|_2}, & \text{if } \|\vec{g}\|_2 < t_l \\ \vec{g} & \text{otherwise} \end{cases}$$

noting that $\|\cdot\|_2$ is the Euclidean norm operator. t_h is the (high) threshold for preventing diverging gradient values while t_l is the (low) threshold for preventing shrinking gradient values. In essence, the above formula is composed of two types of gradient re-scaling. The first part re-projects the gradient to a unit Gaussian ball (“gradient clipping” as prescribed by Pascanu *et al* [9]) when the gradient norm exceeds a threshold $t_h = 1.0$. The second part, on the other hand, is a novel trick we introduce called “gradient boosting”, where, when the norm of the gradient falls below a threshold $t_l = 0.05$, we up-scale it by the factor $\frac{t_l}{\|\vec{g}\|_2}$.

For EXAMM, each neuro-evolution run consisted of 10 islands, each with a population size of 5. New RNNs were generated via intra-island crossover (at a rate of 20%), mutation at a rate 70%, and inter-island crossover at 10% rate. All of EXAMM’s mutation operations (except for *split edge*) were utilized, each chosen with a uniform 10% chance. The experiments labeled *all* were able to select any type of memory cell or Elman neurons at random, each with an equal probability. Each EXAMM run generated 2000 RNNs, with each RNN being trained locally (using the BPTT settings above) for 10 epochs. Recurrent connections that could span a time skip between 1 and 10 could be chosen (uniformly at random). These runs were performed utilizing 20 processors in parallel, and, on average, required approximately 0.5 compute hours. In total, the results we report come from training 10,560,000 RNNs which required ~52,800 CPU hours of compute time.

4.3 Experimental Results

Figure 3 shows the range of the fitness values of the best found neural networks across all of the EXAMM experiments. This combines the results from all folds and all trial repeats – each box in the box plots represent 110 different fitness values. The box plots are ordered according to mean fitness (calculated as mean absolute error, or MAE) of the RNNs for that experiment/setting (across all folds), with the top being the highest average MAE, i.e., the worst performing simulation setting, and the bottom containing the lowest average MAE, i.e., the best performing setting. Means are represented by green triangles and medians by orange bars. Run type names with deep recurrent connections are highlighted in red.

How well the different experiments performed was also analyzed by calculating the mean and standard deviation of all best evolved fitness scores from each repeated experiment across each fold. This was done since each fold of the test data had a different range of potential best results. It was then possible to rank/order the experiments/simulations in terms of their deviation from the mean (providing a less biased metric of improvement). Table 1 presents how well each experiment performed as an average of how many standard deviations they were from the mean in their average case performance. Table 2 is constructed on the same way but this time based on best case performance. Search types which utilized deep recurrent connections (*+rec*) are highlighted in bold.

4.4 Memory Cell Performance

Table 3 shows the frequency of a particular memory cell experiment/setting appearing in the three best (Top 3) or three worst (Bottom 3) slots (in a ranked list) for each prediction parameter for the experiment’s average and best RNN fitness score. The *simple* row includes only the *simple* and *simple+rec* runs and the *all* row includes the *all* and *all+rec* runs, while the other memory cell rows include the *+simple* and *+rec* versions (e.g., the *delta* row includes occurrences of *delta*, *delta+simple*, *delta+rec* and *delta+simple+rec*).

Based on these count results, the Δ -RNN memory cells performed the best, appearing in the top 3 for the average and best cases 4 times each. Furthermore, it did not appear in the bottom 3 for the average and best cases *at all*, making these particular memory cells more reliable than the others. MGU memory cells performed the next best, appearing twice in the average case and 3 times in the best case. However, they also showed up 4 times in the bottom, 3 on the average case, and once in the bottom 3 for the best case networks. Interestingly enough, while the popular LSTM memory cells showed up frequently for the average performance case (3 times), they did not show up at all in the top 3 for the best found RNNs. They also occurred once in the bottom three for average performance and twice in the bottom 3 for best performance.

The experimental results indicate simple neurons performed rather well when combined with deep recurrent connections. The *simple+rec* configuration showed up once in the top 3 for the average case, and twice in the top 3 for the best case. When simple neurons appeared in the bottom 3, it was only in the experiments when no deep recurrent connections were permitted. As a result, aside from the Δ and MGU memory cells, *simple+rec* performed better than the other more complicated memory cells, e.g., LSTM, GRU, and was, furthermore, more reliable than the MGU cells.

The performance of the GRU memory cells was intriguing – they showed up 3 times in the top 3 for the best case RNNs, 0 times for the top 3 average case runs, but 2 and 5 times in the bottom 3 for average and best case networks. This seems to indicate that, while GRU memory cells have the potential to find well performing networks, they are *highly unreliable* for these datasets. We hypothesize that this might due to either high sensitivity to initialization conditions or to unknown limitations in the way they gate/carry temporal information.

Lastly, UGRNN memory cells performed the worst overall. They only appeared once in the top 3 average case and not at all in the top 3 best case. At the same time they occurred 4 and 3 times in the bottom 3 for the average and best case performance rankings.

The *all* configurations did not show up at all in the top 3 or bottom 3, most likely due to the significant size of its particular search space. Given the additional option to select from a large pool of different memory cell types, the EXAMM neuro-evolution procedure might just simply require far more time to decide on optimal cell types that would yield better/top performing networks.

4.5 Effects of Simple Neurons

Table 4 provides measurements for how the addition of simple neurons changed the performance of the varying memory cell types. In it, we show how many standard deviations from the mean the average case moved when averaging the differences of *mgu* to *mgu+simple* and *mgu+rec* to *mgu+simple+rec* (over all four prediction parameters). In the average case, adding simple neurons did appear to yield a modest improvement, improving deviations from the mean

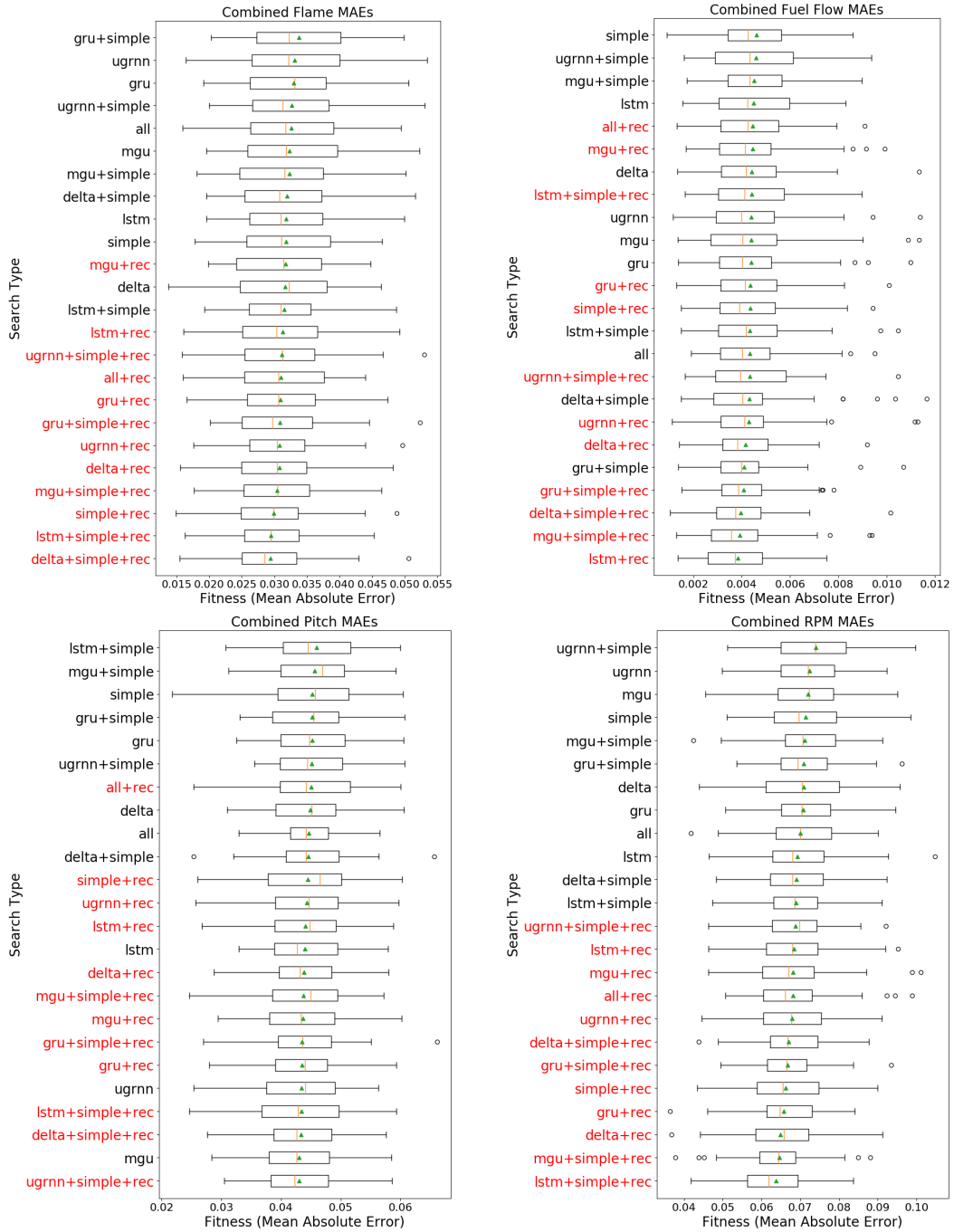


Figure 3: Consolidated range of fitness (mean absolute error) of the best found RNNs for the two datasets’ (flame intensity and fuel flow for the coal plant dataset, and pitch and RPM for the aviation dataset) target prediction parameters. Results are for the 24 experiments across all 6 folds, with 10 repeats per fold. Run types are ordered top-down by mean.

Type	Devs from Mean	Type	Devs from Mean
gru+simple	0.45466	simple	0.21337
gru	0.38537	mgu+simple	0.18593
mgu+simple	0.27395	ugrnn+simple	0.17120
ugrnn+simple	0.26383	all+rec	0.12609
ugrnn	0.24459	lstm	0.11196
all	0.22218	delta	0.08607
mgu	0.21171	lstm+simple+rec	0.07886
lstm+simple	0.05836	mgu+rec	0.07732
delta+simple	0.04819	gru	0.04823
lstm	0.03707	ugrnn	0.04216
simple	0.01420	gru+rec	0.03564
delta	0.00741	simple+rec	0.01922
ugrnn+simple+rec	-0.04944	lstm+simple	0.01803
mgu+rec	-0.05957	mgu	0.00344
lstm+rec	-0.09531	ugrnn+simple+rec	-0.00456
all+rec	-0.10439	all	-0.00649
delta+rec	-0.13052	ugrnn+rec	-0.02236
gru+rec	-0.15598	delta+simple	-0.03849
gru+simple+rec	-0.16988	delta+rec	-0.08420
ugrnn+rec	-0.18138	gru+simple+rec	-0.12883
mgu+simple+rec	-0.20289	gru+simple	-0.13948
simple+rec	-0.30881	delta+simple+rec	-0.22414
lstm+simple+rec	-0.33808	lstm+rec	-0.28345
delta+simple+rec	-0.42524	mgu+simple+rec	-0.28552

(a) σ_{Flame} : Avg MAE		(b) $\sigma_{FuelFlow}$: Avg MAE	
Type	Devs from Mean	Type	Devs from Mean
lstm+simple	0.23909	ugrnn+simple	0.49582
mgu+simple	0.20029	ugrnn	0.32738
ugrnn+simple	0.14481	mgu	0.30650
simple	0.14432	simple	0.26625
gru+simple	0.13351	mgu+simple	0.23401
gru	0.13152	gru+simple	0.20177
delta	0.10322	gru	0.19246
all+rec	0.09201	delta	0.17695
all	0.06990	all	0.10472
delta+simple	0.05982	lstm	0.02485
simple+rec	0.03136	lstm+simple	0.01335
ugrnn+rec	0.00369	delta+simple	0.00523
lstm+rec	-0.03673	ugrnn+simple+rec	-0.00490
lstm	-0.03996	lstm+rec	-0.02911
delta+rec	-0.06630	mgu+rec	-0.06871
mgu+rec	-0.08360	all+rec	-0.08791
mgu+simple+rec	-0.08452	ugrnn+rec	-0.09029
gru+rec	-0.11290	delta+simple+rec	-0.15970
gru+simple+rec	-0.11699	gru+simple+rec	-0.17044
ugrnn	-0.13281	simple+rec	-0.21730
lstm+simple+rec	-0.14307	gru+rec	-0.27053
delta+simple+rec	-0.15425	delta+rec	-0.36819
ugrnn+simple+rec	-0.18647	mgu+simple+rec	-0.40717
mgu	-0.19593	lstm+simple+rec	-0.47505

(c) σ_{Flame} : Avg MAE		(d) σ_{Flame} : Avg MAE	
Type	Devs from Mean	Type	Devs from Mean
lstm+simple	0.23909	ugrnn+simple	0.49582
mgu+simple	0.20029	ugrnn	0.32738
ugrnn+simple	0.14481	mgu	0.30650
simple	0.14432	simple	0.26625
gru+simple	0.13351	mgu+simple	0.23401
gru	0.13152	gru+simple	0.20177
delta	0.10322	gru	0.19246
all+rec	0.09201	delta	0.17695
all	0.06990	all	0.10472
delta+simple	0.05982	lstm	0.02485
simple+rec	0.03136	lstm+simple	0.01335
ugrnn+rec	0.00369	delta+simple	0.00523
lstm+rec	-0.03673	ugrnn+simple+rec	-0.00490
lstm	-0.03996	lstm+rec	-0.02911
delta+rec	-0.06630	mgu+rec	-0.06871
mgu+rec	-0.08360	all+rec	-0.08791
mgu+simple+rec	-0.08452	ugrnn+rec	-0.09029
gru+rec	-0.11290	delta+simple+rec	-0.15970
gru+simple+rec	-0.11699	gru+simple+rec	-0.17044
ugrnn	-0.13281	simple+rec	-0.21730
lstm+simple+rec	-0.14307	gru+rec	-0.27053
delta+simple+rec	-0.15425	delta+rec	-0.36819
ugrnn+simple+rec	-0.18647	mgu+simple+rec	-0.40717
mgu	-0.19593	lstm+simple+rec	-0.47505

Table 1: Average fitness performance values reported for each EXAMM experimental setting. Experimental settings are ranked by their number of standard deviations from the mean of all experiments. Lower values had better performance.

Type	Devs from Mean
gru+simple	-1.02844
mgu+rec	-1.15701
ugrnn+simple	-1.21079
mgu	-1.24655
mgu+simple	-1.26880
gru	-1.29390
simple	-1.30901
lstm+simple	-1.35475
lstm	-1.35496
delta+simple	-1.37473
ugrnn+rec	-1.42362
ugrnn	-1.43371
delta	-1.48912
mgu+simple+rec	-1.55717
gru+simple+rec	-1.58618
lstm+simple+rec	-1.63655
all+rec	-1.64301
all	-1.66893
lstm+rec	-1.70057
ugrnn+simple+rec	-1.71172
gru+rec	-1.73098
delta+rec	-1.95685
simple+rec	-1.97756
delta+simple+rec	-2.08205

(a) σ_{Flame} : Best MAE

Type	Devs from Mean
gru+rec	-1.10116
ugrnn+simple	-1.18567
lstm+simple	-1.18625
mgu+rec	-1.18778
lstm+simple+rec	-1.21500
mgu+simple	-1.21509
all	-1.22138
gru+simple	-1.27796
gru+simple+rec	-1.29070
simple+rec	-1.29699
simple	-1.30479
ugrnn	-1.30559
ugrnn+simple+rec	-1.31366
delta	-1.33034
delta+rec	-1.35481
all+rec	-1.37338
lstm	-1.38003
delta+simple	-1.38368
lstm+rec	-1.38510
ugrnn+rec	-1.42369
mgu	-1.45259
mgu+simple+rec	-1.50962
gru	-1.53812
delta+simple+rec	-1.54667

(b) $\sigma_{FuelFlow}$: Best MAE

Type	Devs from Mean
ugrnn+simple	-0.99073
gru	-1.01889
lstm+simple	-1.09707
gru+simple	-1.10143
delta	-1.19651
lstm	-1.24966
all	-1.25872
delta+rec	-1.42943
mgu+simple	-1.48976
all+rec	-1.55755
ugrnn+rec	-1.58235
mgu+rec	-1.60397
lstm+rec	-1.63888
ugrnn+simple+rec	-1.64192
mgu	-1.67690
ugrnn	-1.70299
delta+simple+rec	-1.77567
delta+simple	-1.78042
gru+rec	-1.81352
lstm+simple+rec	-1.89858
simple	-2.05128
mgu+simple+rec	-2.09451
gru+simple+rec	-2.09545
simple+rec	-2.24764

(c) σ_{Pitch} : Best MAE

Type	Devs from Mean
gru	-0.94516
simple	-0.99991
gru+simple	-1.08121
mgu	-1.17371
ugrnn+simple	-1.19714
all+rec	-1.34347
ugrnn	-1.36917
ugrnn+simple+rec	-1.44366
gru+simple+rec	-1.49508
mgu+simple	-1.49991
lstm	-1.50167
delta+simple+rec	-1.51271
delta+simple	-1.51795
mgu+rec	-1.52494
delta	-1.57259
lstm+simple	-1.64965
all	-1.69526
lstm+simple+rec	-1.71450
ugrnn+rec	-1.72680
lstm+rec	-1.74024
simple+rec	-1.74335
gru+rec	-1.88070
mgu+simple+rec	-1.89718
delta+rec	-2.05063

(d) σ_{RPM} : Best MAE

Table 2: Best fitness performance values reported for each EXAMM experimental setting. Experimental settings are ranked by their number of standard deviations from the mean of all experiments. Lower values had better performance.

Memory Cell	Top 3		Bottom 3	
	Avg	Best	Avg	Best
all	0	0	0	0
simple	1	2	1	1
delta	4	4	0	0
gru	0	3	2	5
lstm	3	0	1	2
mgu	2	3	4	1
ugrnn	1	0	4	3

Table 3: How often a memory cell type appeared in the top 3 or bottom 3 experiments in the best and average cases.

Type	Dev for Avg	Dev for Best
delta	-0.07663	-0.07420
gru	-0.02369	0.04575
lstm	-0.02973	0.02485
mgu	-0.03463	-0.18857
ugrnn	0.07991	0.15908
overall	-0.02365	-0.02018

Table 4: Performance improvement (in std. devs from the mean) for adding simple neurons.

by -0.02 overall, and improving deviation from the mean for all memory cells except for UGRNNs. Adding simple neurons had a similar overall improvement for the best found RNNs, however, this incurred a much wider variance. Despite this variance, 2 of the 3 best found networks had *+simple* as an option, with a third being *simple+rec*. This seems to indicate that most memory cell types could either benefit by mixing/combining them with simple neurons.

4.6 Effects of Deep Recurrent Connections

Table 5 provides similar measurements for EXAMM settings that permitted the addition of deep recurrent edges to the varying memory cell types, as well as the *all* and *simple* runs. Compared to adding *+simple*, the *+rec* setting showed an order of magnitude difference, improving deviations from the mean by -0.2 overall. In addition, for each of the prediction parameters, the best found RNN utilized deep recurrent connections. Looking at the top 3 best and top 3 average case RNNs, 11 out of 12 utilized deep recurrent connections. Similarly, in the bottom 3 best, *+rec* occurs twice and does not appear at all in the bottom 3 average case run types. For the Flame and RPM parameters, on the average case, even the worst performing run type with *+rec* performs better than any experiments without it.

5 Discussion

The results presented in this work contribute some significant and interesting insights for RNN-based time series data prediction. The main findings of this study are as follows:

- *Deep Recurrent Connections*: yielded the most significant improvements in RNN generalization, and, in some cases, were more important than the use of memory cells, i.e., the *simple+rec* experiments performing quite strongly. For all four benchmark datasets, the best found RNNs included those that made use of deep recurrence. As a whole, adding deep recurrent connections to the evolutionary process resulted in large shifts

Type	Dev for Avg	Dev for Best
all	-0.09113	-0.01828
simple	-0.27842	-0.40014
delta	-0.25571	-0.30079
gru	-0.31534	-0.43257
lstm	-0.14463	-0.24462
mgu	-0.11507	0.01901
ugrnn	-0.19291	-0.08625
overall	-0.19903	-0.20909

Table 5: Performance Improvement (in std. devs from the mean) for adding deep recurrent connections.

of improvement in the standard deviations from mean measurement. These results are particularly significant given that the commonly accepted story is that one should primarily use LSTM or other gated neural structures in order to stand a chance at capturing long term time dependencies in temporal data (despite the fact that internal connections only explicitly traverse a single time step) when classically it has been known that time delays and temporal skip connections can vastly improve generalization over sequences.

- *Strong simple+rec Performance:* Another very interesting finding was that only using simple neurons and deep recurrent connections, without any memory cells, (the *simple+rec* experiment) performed quite well. This found the best RNN with respect to the Pitch prediction problem (aviation), the second best on the Flame prediction problem dataset (coal), and the fourth best on the RPM prediction problem (aviation). This shows that, in some cases, it may be more important to have deep recurrent connections than more complicated memory cells.
- *Strong Δ -RNN Memory Cell Performance:* While there is no “free lunch” in statistical learning or optimization [42], the newer Δ -RNN memory cell did consistently stand out as one of the better-performing memory cells. In three out of the four datasets, EXAMM found it to be the best performing RNN cell-of-choice, and for the average case performance, the Δ -RNN made it into the top 3 experiments for all four datasets. Furthermore, unlike the other memory cell experiments Δ -RNN did not appear in the bottom 3 for any of the experiments, either in the average or best cases. The only other experiment setting/configuration to boast top 3 best performance and no bottom 3 performance was the *simple+rec* experiment. However this did not perform as well in the average case, only appearing in the top 3 twice. Our results showing that the Δ -RNN consistently outperforms more complex cells such as the LSTM corroborates the findings of [1], which presented early findings in the domain of language modeling. While a newer memory cell, our results indicate that, while deep recurrence and time delay are critical for robustly modeling sequences, simpler gated cells like the Δ -RNN cell should also be strongly considered when designing RNNs, especially for time series forecasting.

6 Future Work

The choice of selecting time skip depths uniformly at random between the hyperparameter range [1, 10] was a somewhat arbitrary choice. We hypothesize that an adaptive approach to selecting the depth skip (or length of the time delay) based on previously well-performing configurations/model candidates might provide better accuracy and remove the need for choosing the bounds of time delay range. Perhaps the most interesting direction to pursue is to develop memory cells that efficiently and effectively use recurrent connections that explicitly span more than one step in time, i.e., perhaps more intelligent/powerful gating mechanisms could be design to properly mix together the information that flows from multiple time delays. In addition, perhaps EXAMM can be used to automatically incorporate or design better variations of highway connections as well, given the potential expressive power that recurrent highway networks [20] offer.

The strong performance of the *simple+rec* experiment might also suggest that generating and training RNNs using an evolutionary process with Lamarckian weight initialization may make training RNNs with non-gated recurrent connections easier. This naturally happens since neuro-evolution process such as EXAMM will discard poor RNN solutions that occur in the search space, i.e., poor minima/regions that result from exploding or vanishing gradients when using backpropagation through time (BPTT), and not add them to its candidate solution population, preventing the generation of at least offspring that generalize too poorly. As a result, the evolutionary process will tend to preserve RNNs which have been training well (or at least, when trained with BPTT, have well-behaved gradients). Future investigation can explore if this is truly the case by retraining the best found architectures from scratch and comparing their performance across various sequence modeling settings.

7 Conclusion

While most work in the field of neuro-evolution focuses on the evolution of neural architectures that can potentially outperform hand-crafted designs, this work showcases the potential of neuro-evolution for a different use: a robust analysis and investigation of the performance and capabilities of different artificial neural network components. Specifically, we demonstrate EXAMM as powerful tool for analyzing/designing recurrent networks, focused on the choice of internal memory cells and the density and complexity of recurrent connectivity patterns. Rigorously investigating a new neural processing component can be quite challenging given that, often, its performance is tied to the overall architecture it is used within. For most work, new architectural components or strategies are typically only investigated within a few select architectures which may not necessarily represent how well the processing mechanism would perform given a much wider range of potential architectures it could be integrated into. Neuro-evolution helps alleviate this problem by allowing the the structural components themselves to play a key role in determining the architecture/systems they will

most likely work well within. This facilitates a far more fair comparison of their capabilities and, perhaps, allows us to draw more general insights in our quest to construct robust neural models that generalize well.

8 Acknowledgements

This material is in part supported by the U.S. Department of Energy, Office of Science, Office of Advanced Combustion Systems under Award Number #FE0031547 and by the Federal Aviation Administration National General Aviation Flight Information Database (NGAFID) award. We also thank Microbeam Technologies, Inc., as well as Mark Dusenbury, James Higgins, Brandon Wild at the University of North Dakota for their help in collecting and preparing the coal-fired power plant and NGAFID data, respectively.

References

- [1] Alexander G. Ororbia II, Tomas Mikolov, and David Reitter. Learning simpler language models with the differential state framework. *Neural Computation*, 0(0):1–26, 2017. PMID: 28957029.
- [2] Junyoung Chung, Caglar Gulcehre, KyungHyun Cho, and Yoshua Bengio. Empirical evaluation of gated recurrent neural networks on sequence modeling. *arXiv preprint arXiv:1412.3555*, 2014.
- [3] Sepp Hochreiter and Jürgen Schmidhuber. Long short-term memory. *Neural Computation*, 9(8):1735–1780, 1997.
- [4] Guo-Bing Zhou, Jianxin Wu, Chen-Lin Zhang, and Zhi-Hua Zhou. Minimal gated unit for recurrent neural networks. *International Journal of Automation and Computing*, 13(3):226–234, 2016.
- [5] Jasmine Collins, Jascha Sohl-Dickstein, and David Sussillo. Capacity and trainability in recurrent neural networks. *arXiv preprint arXiv:1611.09913*, 2016.
- [6] Yoshua Bengio, Paolo Frasconi, and Patrice Simard. The problem of learning long-term dependencies in recurrent networks. In *IEEE international conference on neural networks*, pages 1183–1188. IEEE, 1993.
- [7] Yoshua Bengio, Patrice Simard, and Paolo Frasconi. Learning long-term dependencies with gradient descent is difficult. *IEEE transactions on neural networks*, 5(2):157–166, 1994.
- [8] Sepp Hochreiter, Yoshua Bengio, Paolo Frasconi, Jürgen Schmidhuber, et al. Gradient flow in recurrent nets: the difficulty of learning long-term dependencies, 2001.
- [9] Razvan Pascanu, Tomas Mikolov, and Yoshua Bengio. On the difficulty of training recurrent neural networks. In *International Conference on Machine Learning*, pages 1310–1318, 2013.
- [10] Li Jing, Caglar Gulcehre, John Peurifoy, Yichen Shen, Max Tegmark, Marin Soljacic, and Yoshua Bengio. Gated orthogonal recurrent units: On learning to forget. *Neural computation*, 31(4):765–783, 2019.
- [11] Tsungnan Lin, Bill G Horne, Peter Tino, and C Lee Giles. Learning long-term dependencies in narx recurrent neural networks. *IEEE Transactions on Neural Networks*, 7(6):1329–1338, 1996.
- [12] Tsungnan Lin, Bill G Horne, and C Lee Giles. How embedded memory in recurrent neural network architectures helps learning long-term temporal dependencies. *Neural Networks*, 11(5):861–868, 1998.
- [13] Tsungnan Lin, Bill G Horne, C Lee Giles, and Sun-Yuan Kung. What to remember: How memory order affects the performance of narx neural networks. In *1998 IEEE International Joint Conference on Neural Networks Proceedings. IEEE World Congress on Computational Intelligence (Cat. No. 98CH36227)*, volume 2, pages 1051–1056. IEEE, 1998.
- [14] C Lee Giles, Tsungnan Lin, Bill G Horne, and Sun-Yuan Kung. The past is important: a method for determining memory structure in narx neural networks. In *1998 IEEE International Joint Conference on Neural Networks Proceedings. IEEE World Congress on Computational Intelligence (Cat. No. 98CH36227)*, volume 3, pages 1834–1839. IEEE, 1998.
- [15] Eugen Diaconescu. The use of narx neural networks to predict chaotic time series. *Wseas Transactions on computer research*, 3(3):182–191, 2008.
- [16] James L McClelland, David E Rumelhart, PDP Research Group, et al. *Parallel distributed processing*, volume 2. MIT press Cambridge, MA:, 1987.
- [17] Kaiming He, Xiangyu Zhang, Shaoqing Ren, and Jian Sun. Deep residual learning for image recognition. In *Proceedings of the IEEE conference on computer vision and pattern recognition*, pages 770–778, 2016.
- [18] Alex Graves. Generating sequences with recurrent neural networks. *arXiv preprint arXiv:1308.0850*, 2013.

- [19] Rupesh Kumar Srivastava, Klaus Greff, and Jürgen Schmidhuber. Highway networks. *arXiv preprint arXiv:1505.00387*, 2015.
- [20] Julian Georg Zilly, Rupesh Kumar Srivastava, Jan Koutník, and Jürgen Schmidhuber. Recurrent highway networks. In *Proceedings of the 34th International Conference on Machine Learning-Volume 70*, pages 4189–4198. JMLR.org, 2017.
- [21] Jinmiao Chen and Narendra S Chaudhari. Segmented-memory recurrent neural networks. *IEEE transactions on neural networks*, 20(8):1267–1280, 2009.
- [22] AbdElRahman ElSaid, Brandon Wild, James Higgins, and Travis Desell. Using lstm recurrent neural networks to predict excess vibration events in aircraft engines. In *2016 IEEE 12th International Conference on e-Science (e-Science)*, pages 260–269. IEEE, 2016.
- [23] AbdElRahman ElSaid, Fatima El Jamiy, James Higgins, Brandon Wild, and Travis Desell. Using ant colony optimization to optimize long short-term memory recurrent neural networks. In *Proceedings of the Genetic and Evolutionary Computation Conference*, pages 13–20. ACM, 2018.
- [24] Alexander Ororbia, AbdElRahman ElSaid, and Travis Desell. Investigating recurrent neural network memory structures using neuro-evolution. In *Proceedings of the Genetic and Evolutionary Computation Conference, GECCO '19*, pages 446–455, New York, NY, USA, 2019. ACM.
- [25] David E Goldberg and John H Holland. Genetic algorithms and machine learning. *Machine learning*, 3(2):95–99, 1988.
- [26] Khalid Salama and Ashraf M Abdelbar. A novel ant colony algorithm for building neural network topologies. In *Swarm Intelligence*, pages 1–12. Springer, 2014.
- [27] Masanori Suganuma, Shinichi Shirakawa, and Tomoharu Nagao. A genetic programming approach to designing convolutional neural network architectures. In *Proceedings of the Genetic and Evolutionary Computation Conference, GECCO '17*, pages 497–504, New York, NY, USA, 2017. ACM.
- [28] Yanan Sun, Bing Xue, and Mengjie Zhang. Evolving deep convolutional neural networks for image classification. *CoRR*, abs/1710.10741, 2017.
- [29] Risto Miikkulainen, Jason Liang, Elliot Meyerson, Aditya Rawal, Dan Fink, Olivier Francon, Bala Raju, Hormoz Shahrzad, Arshak Navruzyan, Nigel Duffy, and Babak Hodjat. Evolving deep neural networks. *arXiv preprint arXiv:1703.00548*, 2017.
- [30] Kenneth Stanley and Risto Miikkulainen. Evolving neural networks through augmenting topologies. *Evolutionary computation*, 10(2):99–127, 2002.
- [31] Kenneth O Stanley, David B D’Ambrosio, and Jason Gauci. A hypercube-based encoding for evolving large-scale neural networks. *Artificial life*, 15(2):185–212, 2009.
- [32] Aditya Rawal and Risto Miikkulainen. Evolving deep lstm-based memory networks using an information maximization objective. In *Proceedings of the Genetic and Evolutionary Computation Conference 2016*, pages 501–508. ACM, 2016.
- [33] Aditya Rawal and Risto Miikkulainen. From nodes to networks: Evolving recurrent neural networks. *CoRR*, abs/1803.04439, 2018.
- [34] Andrés Camero, Jamal Toutouh, and Enrique Alba. Low-cost recurrent neural network expected performance evaluation. *arXiv preprint arXiv:1805.07159*, 2018.
- [35] Andrés Camero, Jamal Toutouh, and Enrique Alba. A specialized evolutionary strategy using mean absolute error random sampling to design recurrent neural networks. *arXiv preprint arXiv:1909.02425*, 2019.
- [36] Travis Desell, Sophine Clachar, James Higgins, and Brandon Wild. Evolving deep recurrent neural networks using ant colony optimization. In *European Conference on Evolutionary Computation in Combinatorial Optimization*, pages 86–98. Springer, 2015.
- [37] AbdElRahman ElSaid, Fatima El Jamiy, James Higgins, Brandon Wild, and Travis Desell. Optimizing long short-term memory recurrent neural networks using ant colony optimization to predict turbine engine vibration. *Applied Soft Computing*, 2018.
- [38] David E Rumelhart, Geoffrey E Hinton, Ronald J Williams, et al. Learning representations by back-propagating errors. *Cognitive modeling*, 5(3):1, 1988.
- [39] AbdElRahman ElSaid, Steven Benson, Shuchita Patwardhan, David Stadem, and Desell Travis. Evolving recurrent neural networks for time series data prediction of coal plant parameters. In *The 22nd International Conference on the Applications of Evolutionary Computation*, Leipzig, Germany, April 2019.

- [40] Paul J Werbos. Backpropagation through time: what it does and how to do it. *Proceedings of the IEEE*, 78(10):1550–1560, 1990.
- [41] Rafal Jozefowicz, Wojciech Zaremba, and Ilya Sutskever. An empirical exploration of recurrent network architectures. In *International Conference on Machine Learning*, pages 2342–2350, 2015.
- [42] David H Wolpert, William G Macready, et al. No free lunch theorems for optimization. *IEEE transactions on evolutionary computation*, 1(1):67–82, 1997.